

Supporting Information

Variable autoinhibition among deafness-associated variants of Diaphanous 1 (DIAPH1)

Rabina Lakha¹, Angela M. Montero¹, Tayyaba Jabeen¹, Christina C. Costeas¹, Jia Ma², Christina

L. Vizcarra^{1,*}

¹ Department of Chemistry, Barnard College, New York, NY USA

² Department of Chemistry, Columbia University, New York, NY USA

* email: cvizcarr@barnard.edu

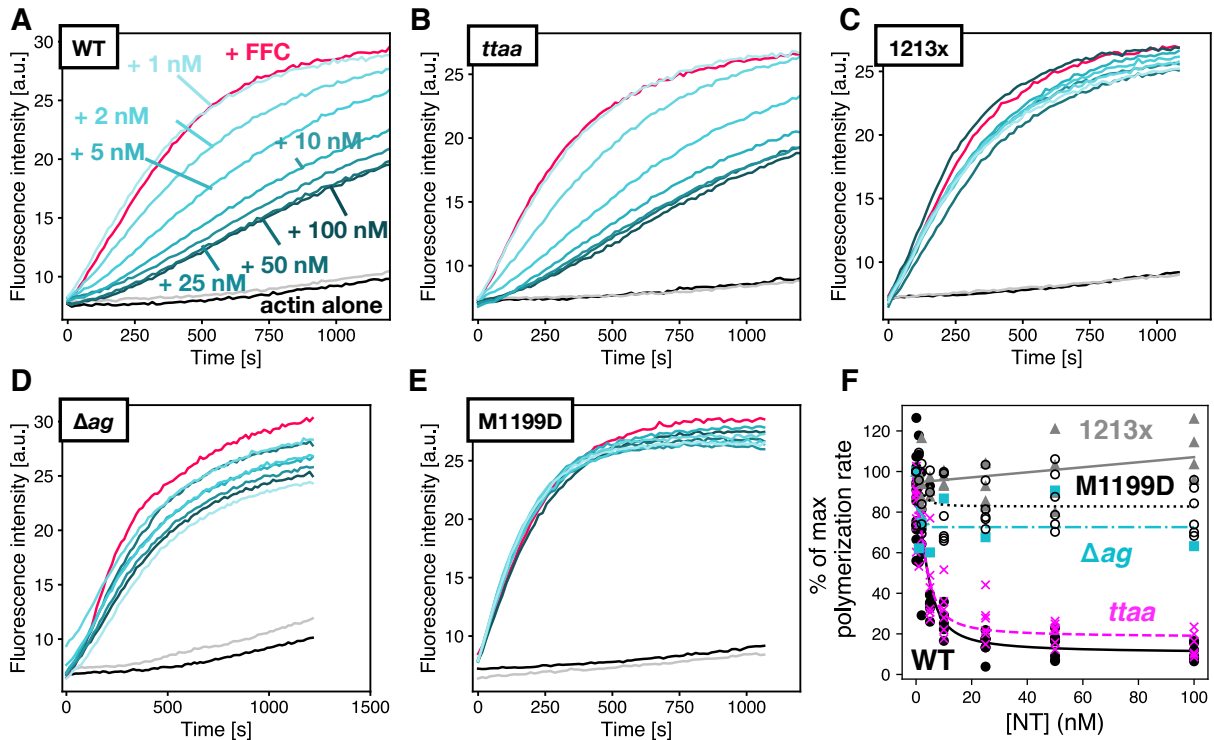


Figure S1. Varied auto inhibition of DIAPH1-FFC mutants by INF2-NT. Pyrene-actin assembly assays were carried out with 2 μ M actin (5% pyrene-labeled), \pm 5 nM of FFC, either (A) WT; (B) *ttaa*; (C) 1213x; (D) Δag ; or (E) M1199D, with varied concentration of INF2-NT. Concentrations of NT are indicated in (A), and the color scheme is the same in panels (B-E), with actin plus 200 nM NT and no FFC in gray. (F) Inhibition curves were calculated from the slopes of raw pyrene traces at 100 s and fit with a quadratic binding model that assumes 1:1 binding between dimers.

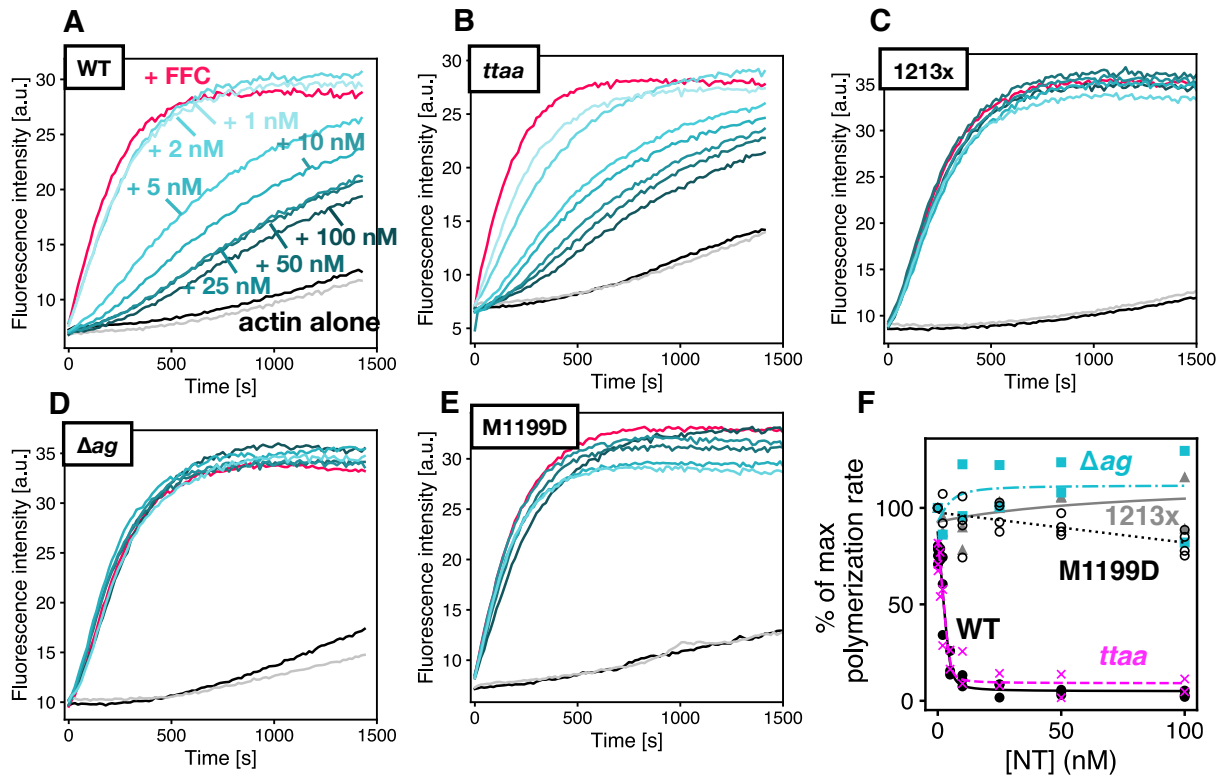


Figure S2. Varied auto inhibition of DIAPH1-FFC mutants. Replicate of Figure 4 with different protein preparations. Pyrene-actin assembly assays were carried out with 2 μ M actin (5% pyrene-labeled), \pm 5 nM of FFC, either (A) WT; (B) *ttaa*; (C) 1213x; (D) Δag ; or (E) M1199D, with varied concentration of WT DIAPH1-NT. Concentrations of NT are indicated in (A), and the color scheme is the same in panels (B-E), with actin plus 200 nM NT and no FFC in gray. (F) Inhibition curves were calculated from the slopes of raw pyrene traces at 100 s and fit with a quadratic binding model that assumes 1:1 binding between dimers.

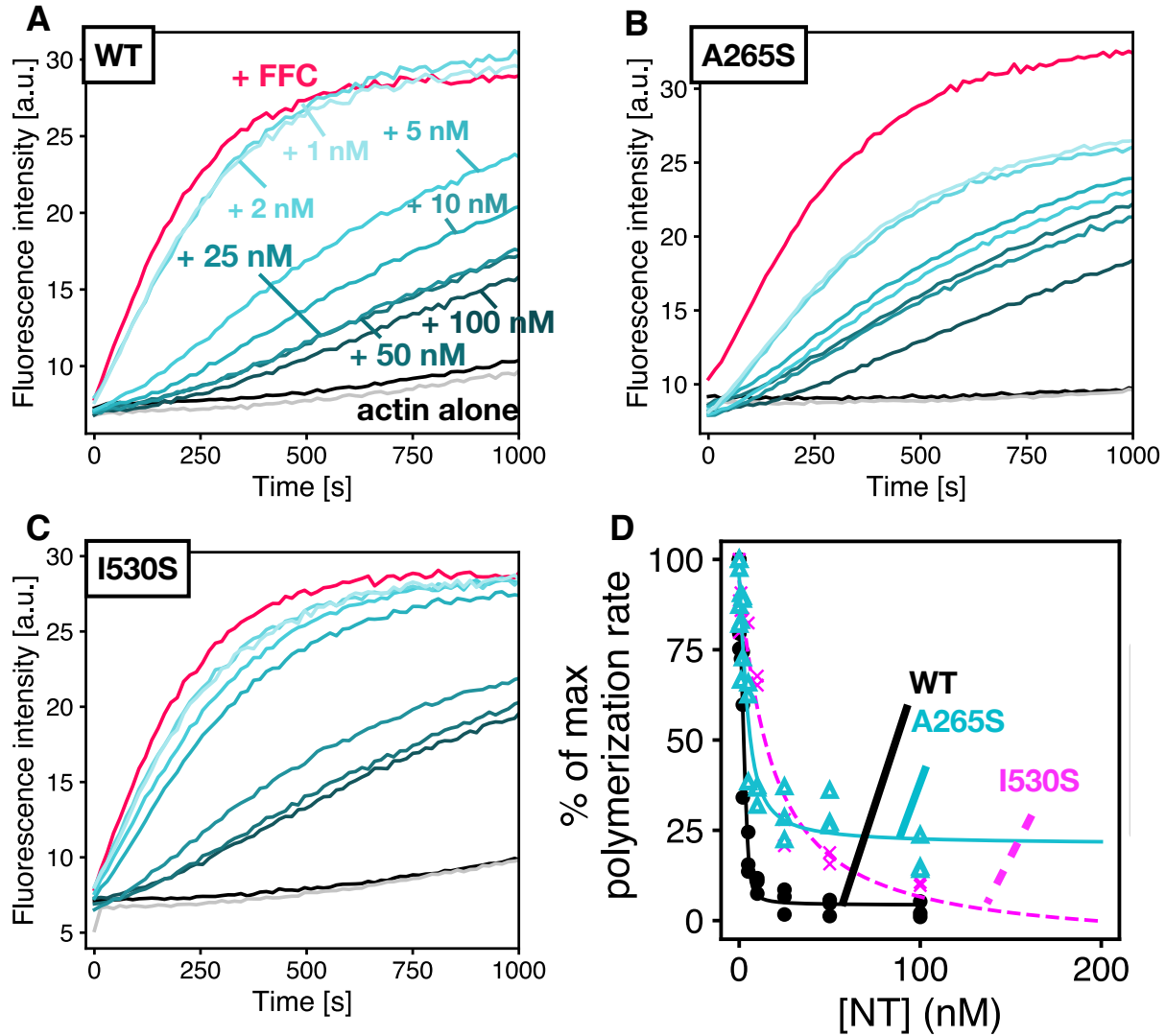


Figure S3. Auto inhibition by DIAPH1-NT mutants. *Replicate of data in Figure 5 with different protein preparations.* Pyrene-actin assembly assays were carried out with 2 μ M actin (5% pyrene-labeled), \pm 5 nM of WT-FFC, titrated with either (A) WT; (B) A265S; or (C) I530S DIAPH1-NT. Concentrations of NT are indicated in (A), and the color scheme is the same in panels (B,C), with actin plus 200 nM NT (no FFC) in gray. (D) Inhibition curves were calculated from the slopes of raw pyrene traces at 100 s and fit with a quadratic binding model that assumes 1:1 binding between dimers.

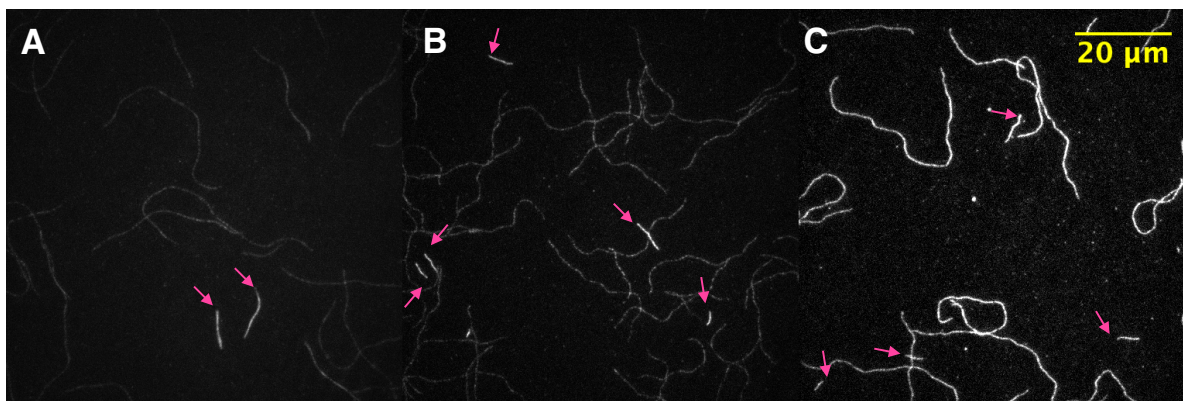


Figure S4. Differential effects of cysteine-labeling on profilin isoforms. Total internal reflection fluorescence (TIRF) microscopy of 1 μM rabbit skeletal muscle actin (15% Cy3B-labeled on Cys374), 2 nM formin-FFC (*Drosophila* Cappuccino), and 2.5 μM profilin: (A) human profilin1, (B) *Drosophila* profilin (chickadee), (C) *S. pombe* profilin. Each panel shows a snapshot from a TIRF movie at 10-20 minutes after the addition of polymerization buffer. Slow-growing filaments are indicated by pink arrows, and are presumed not to be formin-bound. In the presence of *S. pombe* profilin, the formin-elongated filaments (unmarked) are of similar brightness to the slow-growing filaments. Actin was labeled with Cy3B-maleimide as described Chen et al.¹ Cappuccino-FFC was purified and TIRF experiments were carried out as in Vizcarra et al.² Profilin isoforms were purified as in Bor et al.³

References

- (1) Chen, C. K., Sawaya, M. R., Phillips, M. L., Reisler, E. & Quinlan, M. E. Multiple Forms of Spire-Actin Complexes and their Functional Consequences. *J. Biol. Chem.* **2012**, 287 (13), 10684. <https://doi.org/10.1074/jbc.M111.317792>
- (2) Vizcarra, C. L., Bor, B. & Quinlan, M. E. The Role of Formin Tails in Actin Nucleation, Processive Elongation, and Filament Bundling. *J. Biol. Chem.* **2014**, 289 (44), 30602. <https://doi.org/10.1074/jbc.M114.588368>
- (3) Bor, B., Vizcarra, C. L., Phillips, M. L. & Quinlan, M. E. Autoinhibition of the formin Cappuccino in the absence of canonical autoinhibitory domains. *Mol. Biol. Cell* **2012**, 23 (19), 3801. <https://doi.org/10.1091/mbc.e12-04-0288>